AGU PUBLICATIONS

JGR

Journal of Geophysical Research: Space Physics

RESEARCH ARTICLE

10.1002/2015JA022264

ELF/VLF wave propagation at subauroral latitudes: Conjugate observation between the ground and Van Allen Probes A

Claudia Martinez-Calderon[1], Kazuo Shiokawa[1], Yoshizumi Miyoshi[1], Kunihiro Keika[1], Mitsunori Ozaki[2], Ian Schofield[3], Martin Connors[3], Craig Kletzing[4], Miroslav Hanzelka[5,6], Ondrej Santolik[5,6], and William S. Kurth[4]

[1]Institute for Space-Earth Environmental Research, Nagoya University, Nagoya, Japan, [2]Faculty of Electrical and Computer Engineering, Institute of Science and Engineering, Kanazawa University, Kanazawa, Japan, [3]Athabasca University Observatories, Athabasca, Alberta, Canada, [4]Department of Physics and Astronomy, University of Iowa, Iowa City, Iowa, USA, [5]Faculty of Mathematics and Physics, Charles University, Prague, Czech Republic, [6]Institute of Atmospheric Physics, Czech Academy of Sciences, Prague, Czech Republic

Key Points:
- Conjugate observation of QP emission and accompanying short pulse between satellite and ground
- Time delay analysis shows QP observed first at ATH while short pulse observed first by RBSP A
- We successfully reproduced propagation of QP using in situ cold plasma density profile by RBSP A

Correspondence to:
C. Martinez-Calderon,
claudia@isee.nagoya-u.ac.jp

Citation:
Martinez-Calderon, C., et al. (2016), ELF/VLF wave propagation at subauroral latitudes: Conjugate observation between the ground and Van Allen Probes A, *J. Geophys. Res. Space Physics*, *121*, 5384–5393, doi:10.1002/2015JA022264.

Received 11 DEC 2015
Accepted 26 MAY 2016
Accepted article online 1 JUN 2016
Published online 28 JUN 2016

Abstract We report simultaneous observation of ELF/VLF emissions, showing similar spectral and frequency features, between a VLF receiver at Athabasca (ATH), Canada, ($L = 4.3$) and Van Allen Probes A (Radiation Belt Storm Probes (RBSP) A). Using a statistical database from 1 November 2012 to 31 October 2013, we compared a total of 347 emissions observed on the ground with observations made by RBSP in the magnetosphere. On 25 February 2013, from 12:46 to 13:39 UT in the dawn sector (04–06 magnetic local time (MLT)), we observed a quasiperiodic (QP) emission centered at 4 kHz, and an accompanying short pulse lasting less than a second at 4.8 kHz in the dawn sector (04–06 MLT). RBSP A wave data showed both emissions as right-hand polarized with their Poynting vector earthward to the Northern Hemisphere. Using cross-correlation analysis, we did, for the first time, time delay analysis of a conjugate ELF/VLF event between ground and space, finding +2 to +4 s (ATH first) for the QP and −3 s (RBSP A first) for the pulse. Using backward tracing from ATH to the geomagnetic equator and forward tracing from the equator to RBSP A, based on plasmaspheric density observed by the spacecraft, we validate a possible propagation path for the QP emission which is consistent with the observed time delay.

1. Introduction

Extremely low (ELF) and very low (VLF) frequency waves are two of the most common naturally occurring plasma waves. They propagate in the whistler mode along the geomagnetic field lines, away from their source near the equatorial region of the magnetosphere [e.g., *Lauben et al.*, 2002]. These waves have been previously classified according to their spectral features and include, among others, emissions which are incoherent like hiss, discrete such as chorus, or periodic or quasiperiodic [*Helliwell*, 1965]. As these waves propagate, they can resonate with energetic particles in the radiation belts, regulating the electron population and thus playing a significant role in radiation belt dynamics [e.g., *Meredith et al.*, 2003; *Miyoshi et al.*, 2003, 2015; *Horne et al.*, 2005; *Lyons et al.*, 1972; *Bortnik and Thorne*, 2007; *Němec et al.*, 2014; *Hayosh et al.*, 2013].

Since the 1950s, there have been several experiments and theoretical studies on ELF wave and VLF wave propagation, as comprehensively reviewed by *Barr et al.* [2000]. Even though waves can propagate over long distances, they are believed to still contain information regarding their emission and generation mechanisms. Therefore, by using the characteristics of ELF/VLF waves in remote locations, we can try to deduce the properties of wave/particle generation mechanisms. Using the POLAR/PWI wideband receiver, *Lauben et al.* [2002] found that the propagation of chorus waves can remain parallel to the geomagnetic field lines, indicating that even in the absence of field-aligned cold plasma density enhancements, there are sufficient favorable conditions for wave particle interactions. Using simultaneous observations made by four Cluster spacecrafts near the geomagnetic equator during a geomagnetically disturbed period, *Santolik et al.* [2003a] analyzed the propagation and time-frequency properties of nighttime chorus. They found a similar propagation direction from observed time-frequency delays and from Poynting flux calculations based on electric and magnetic measurements. Using ray tracing analysis, *Chum and Santolík* [2005] and *Santolík et al.* [2006] studied the trajectories of chorus waves propagating obliquely and the possibility of divergence of the wave normal angle during these trajectories. They found that deviation of the initial wave vector from the magnetic field line can

determine if the wave is more likely to reach the ground or be reflected into the plasmasphere, contributing to plasmaspheric hiss, or into the magnetosphere. None of these previous studies of ELF/VLF wave propagation observed by satellites compared their observations with ground-based measurements. Recently, *Titova et al.* [2015] observed a conjugate quasiperiodic (QP) event, during a substorm, between the ground station of Kannuslehto, Northern Finland, ($L = 5.3$), and Radiation Belt Storm Probes (RBSP) A. QP are wideband whistler mode waves in the very low frequency (VLF) range, characterized by a periodic modulation of their wave intensity, usually longer than the two-hop whistler group delay [e.g., *Helliwell*, 1965; *Kitamura et al.*, 1968]. They are mostly observed on the dayside [e.g., *Sato et al.*, 1974; *Martinez-Calderon et al.*, 2015b], lasting from a few minutes to several hours and with periods of several seconds to minutes [e.g., *Hayosh et al.*, 2014]. They have been divided into two categories, type 1 if they are found to be related to geomagnetic pulsations with a similar time period and type 2 if the emissions have no correlation [e.g., *Sazhin and Hayakawa*, 1994; *Kitamura et al.*, 1968; *Sato et al.*, 1974]. *Titova et al.* [2015] used wave measurements to calculate the probable location of the source of the emission (at $L \sim 4$) and determine that the slow variations in frequency range and drift are of a temporal nature. They focused particularly on the characteristics of the source region and on the evolution of the energy and pitch angle of the energetic electrons observed simultaneously on board RBSP A and did not discuss the propagation properties of the observed QP emission.

In this study, we present a VLF/ELF event showing a QP emission simultaneously observed on the ground by a VLF receiver located at subauroral latitudes in Athabasca (Canada) and in space by RBSP A on 25 February 2013. Our goal is to use this rare event to study the propagation properties of a VLF/ELF emission at subauroral latitudes, from the inner magnetosphere where RBSP A was located, all the way to the ground station of ATH. Making use of in situ observations from both locations, satellite and ground, we performed wave and propagation analyses, presenting the first results of a time delay analysis and subsequent ray tracing simulations between these two locations. We have successfully reproduced the observations using ray tracing with a cold plasma density distribution evaluated from RBSP A data. We show that the ray tracing can explain the observed time delay. The resulting solution highlights the importance of the plasma density distribution solution in the propagation of the observed QP emission.

2. Observations

Ground-based measurements were made with a delta-type loop antenna located at subauroral latitudes at the Athabasca University Geophysical Observatory (54.60°N, 246.36°E, magnetic latitude (MLAT) = 61.2°N, $L = 4.3$). The receiver has two cross vertical loops, each with 10 turns and a 16 m^2 area, providing the north-south and east-west magnetic field variations with a high sampling rate of 100 kHz. These data are recorded continuously at 10 min intervals along with riometer data and GPS time signal with a 1 μs accuracy. More details on this system are explained by *Ozaki et al.* [2008], *Shiokawa et al.* [2014], and *Martinez-Calderon et al.* [2015a].

We used both survey and continuous waveform burst mode data from the Electric and Magnetic Field Instrument Suite and Integrated Science (EMFISIS) waves instrument on board RBSP A [*Kletzing et al.*, 2013]. The survey mode includes a high-frequency spectrum and a set of spectral matrices containing the three axis correlations of the electric and magnetic field components every 6 s bin averaged between 2 Hz and 12 kHz. The continuous burst mode provides, in addition to the standard set of matrices, continuous waveforms for 5.968 s between each 6 s survey data set. This data set allowed us to obtain power spectral density and multicomponent wave analysis of ELF/VLF events. To obtain in situ cold plasma density at the time of the observation, we measured the upper hybrid resonance band using the electric field data from the high-frequency receiver (HFR) of EMFISIS [*Kurth et al.*, 2015].

Using a database of ELF/VLF emissions observed at ATH, from 1 November 2012 to 31 October 2013 [*Martinez-Calderon et al.*, 2015b], we compared the waves observed on the ground with those observed in the magnetosphere by the RBSP A and RBSP B. During a 1 year period, ATH observed a total of 347 ELF/VLF emissions, with 77 cases of which the footprints of RBSP A and/or B were located within 1000 km from ATH. These possible conjugate cases were found using the Conjunction Event Finder of *Miyashita et al.* [2011]. However, only a single case showed the same spectral and frequency features both at ATH and RBSP A.

2.1. Conjugate Observation

From 12:46 to 13:39 UT on 25 February 2013, a clear quasiperiodic (QP) emission centered around 4 kHz was observed simultaneously at ATH and by RBSP A. Figure 1 shows a 10 min interval from 13:00 UT to 13:10 UT

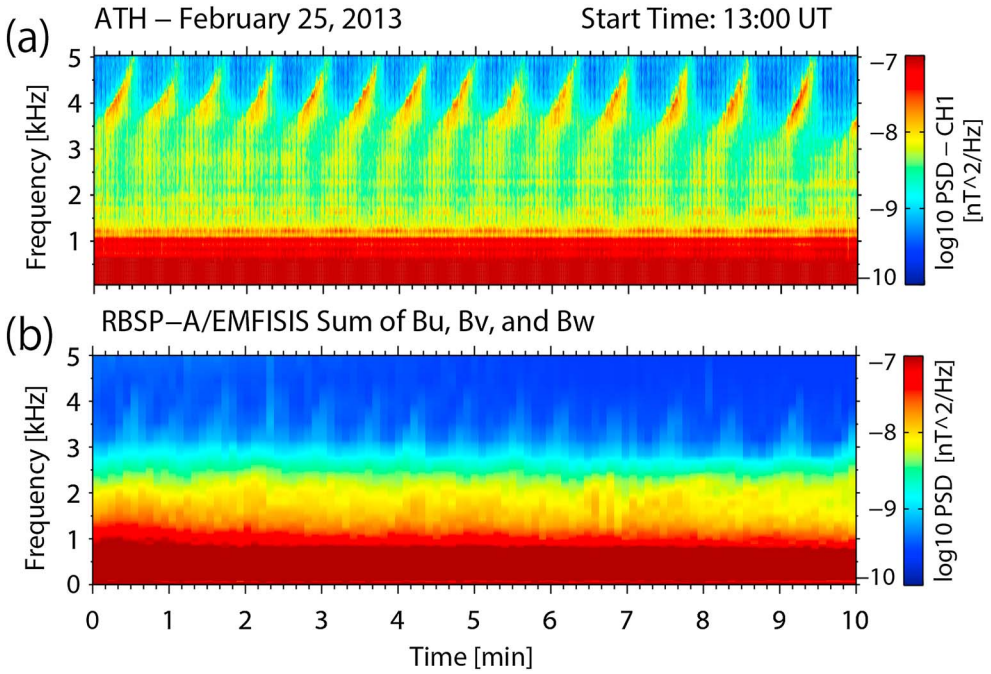

Figure 1. Power spectral density of the quasiperiodic event observed on 25 February 2013 from 12:46 to 13:39 UT. A 10 min snippet of the QP emission observed at (a) ATH and (b) RBSP A (survey mode).

during this conjugate event. The power spectral density (PSD) from 0 to 5 kHz as seen by the receiver at ATH is shown in Figure 1a and as seen by the EMFISIS wave instrument on board RBSP A (survey mode) in Figure 1b. B_u, B_v, and B_w are the magnetic field components in the UVW scientific coordinate system aligned with the EFW booms of the satellite, with *w* being the spin axis [*Kletzing et al.*, 2013]. Both figures show the emission centered at ~4 kHz with a periodicity of 25–40 s and with a one to one correspondence of the QP elements. We note that the wave intensity at ATH is approximately 1 to 2 orders of magnitude stronger compared to RBSP A. A polarization analysis showed that the emission at ATH was strongly right-hand polarized and thus directly incoming from the ionosphere without reflection. At the time of the event, Pc4 and Pc5 geomagnetic pulsations were observed on the rapid-run magnetograms (4 s averages) from the induction magnetometer (64 Hz sampling) located at ATH and nearby fluxgate magnetometers.

Figure 2a gives the geographic location of ATH (red triangle) and the footprint of RBSP A (blue line) during the conjugate event. At the closest point, corresponding to 12:46 UT, both locations were separated by approximately 300 km and at the farthest point, at 13:39UT, by 1270 km. During the event, ATH and RBSP A were on the dawnside. Figures 2b and 2c give the position and direction of RBSP A (blue line) during the conjugate event from 12:46 to 13:39 UT as function of the geocentric solar magnetospheric (GSM) coordinate system. Figure 2b shows the meridional plane, while Figure 2c shows the equatorial plane. RBSP A was located inward ($L = 3.65$) from the field line of ATH ($L = 4.3$) and approximately 11° north of the geomagnetic equator. The position of ATH is marked by a red triangle in both figures: both the ground station and the satellite were on the dawnside. Using the frequency of the upper hybrid resonance provided by the EMFISIS HFR (not shown), we determined that RBSP A was passing through or inside of the plasmapause at the time of the observation.

The intensity of the event triggered RBSP A to capture 54 s of continuous waveform burst mode providing high time resolution samples from all three axes of magnetic field sensors. Figure 3 shows the resulting PSD calculated from the (a) EMFISIS waveforms and from (b) ATH data, for frequencies between 3 and 5 kHz, for a total observation period of 60 s. On both figures, we observe the same QP element spanning approximately 30 s and centered at 4.1 kHz. We note that there is another emission at higher frequencies, a short pulse (SP) lasting less than a second, between 4.5 and 5 kHz, that is also visible at both locations. This pulse can be seen at approximately the 51 s mark for RBSP and at the 52 s mark for ATH, as indicated by the magenta arrows. The SP does not seem to be a whistler since there is no frequency dispersion. It could possibly be a triggered emission, but we are unable to corroborate its origins at this time. However, we are interested in the fact that it

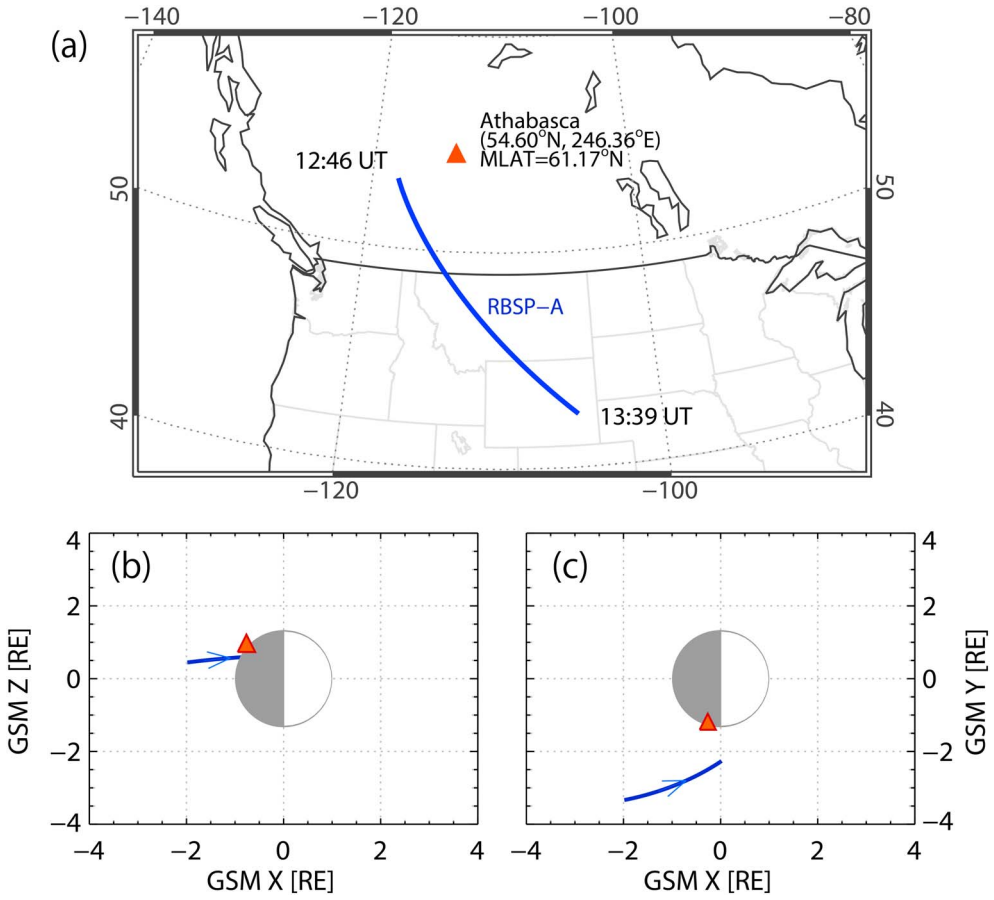

Figure 2. (a) Map showing the location of the ground station of ATH (red triangle) and the footprint of RBSP A (blue line) at the moment of the conjugate event. (b and c) The location of RBSP A in the magnetosphere.

was detected at both locations together with the main QP emission, improving the validity of the propagation analysis.

2.2. Propagation Analysis

Using the electric and magnetic field components from the continuous burst data and initial intensity of the magnetic field (B_0) from the flux gate magnetometer of the EMFISIS instrument, we made a wave propagation analysis. We found that the QP and the SP shared the same characteristics: both were right-hand polarized and had a planarity close to ~25% (not shown for brevity). Figure 3c shows the results of the angle between the Poynting vector and $\vec{B}_0$, giving an indication of the wave propagation when it encountered RBSP A. We calculated the Poynting vector from the EB cross spectra as described by *Santolik et al.* [2001]. We note that the gap shown in this figure around 4 kHz is due to an interference line in the electrical field data measurements used to determine the Poynting flux. Both the QP element and the SP are in blue indicating that the Poynting vector is parallel to the magnetic field, meaning earthward toward the Northern Hemisphere. Figure 3d shows, in the same format, the angle between the wave vector $\vec{k}$ and $\vec{B}_0$, with $\theta_{Bk} = 0°$ for both parallel and antiparallel directions with respect to $\vec{B}_0$. We estimated the wave vector from the singular value decomposition of the spectral matrices as detailed in *Santolík et al.* [2003b]. The QP shows a wave angle close to $\theta_{Bk} = 40° \sim 50°$ with slightly lower values for SP. This is in agreement with previous results suggesting that as the wave gets farther away from the source, the wave vectors gradually deviate from the $\vec{B}_0$ direction reaching oblique angles of up to 60° at ±10° above and below the magnetic equator [e.g., *Santolik et al.*, 2003a]. We would like to note that even though survey mode data were available between 12:55 UT and 13:40 UT, the QP was very weak; thus, we have decided to concentrate on the Poynting and wave vector information from the burst mode.

To have more information on wave propagation from the magnetosphere to the ground, we performed a cross-correlation analysis that allowed us to estimate the degree of correlation between the signals from

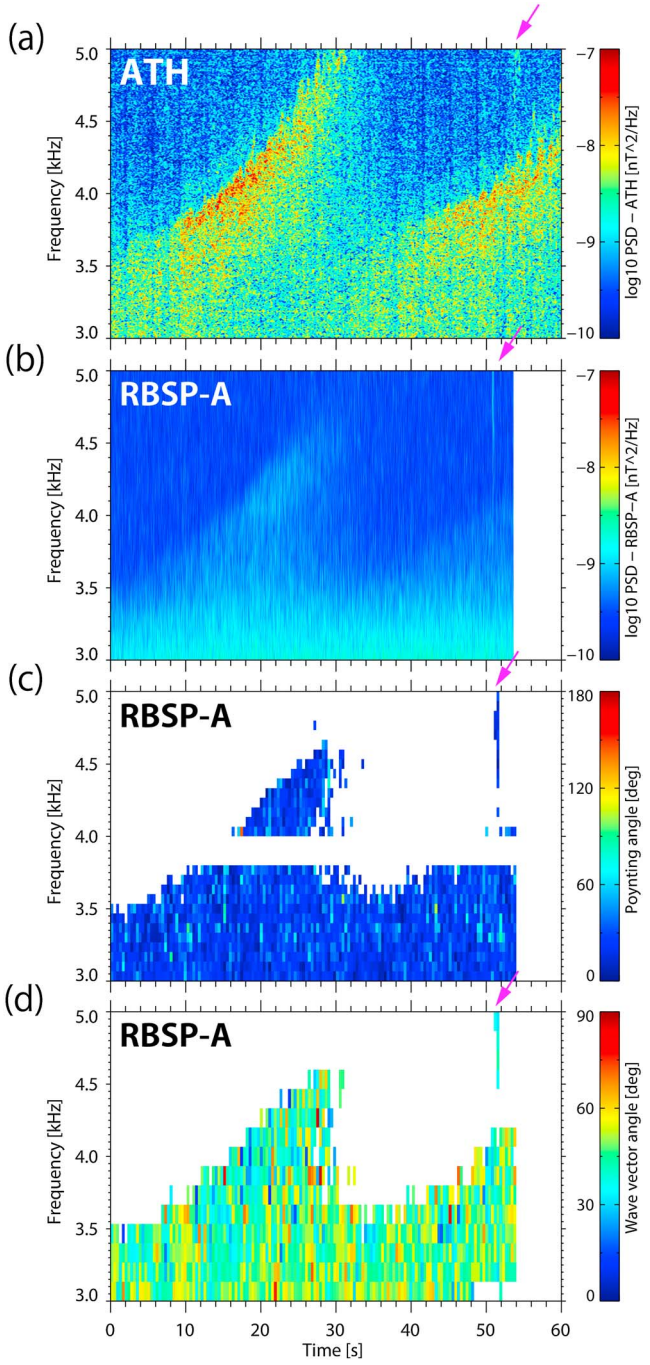

Figure 3. One minute close-up of a QP element observed on 25 February 2013 from 13:00 to 13:01 UT, showing spectra at (a) ATH and (b) RBSP A (54 s of burst mode), as well as (c) Poynting and (d) wave vector angles. Magenta arrows indicate the position of the short pulse in all panels.

ATH and RBSP A as a function of the time delay between them, as shown in Figure 4. The maximum of the cross-correlation function gives the time delay (lag) for which the two signals are the best aligned: the location of the maximum of the correlation coefficient being positive (negative) means that ATH (RBSP A) saw the emission first. Since the signal from RBSP A has a lower sampling rate of 35 kHz, we interpolated both in frequency and time to match the 100 kHz sampling rate of ATH. In the case of the QP element, we calculated the time delay by shifting the QP element for the (1) full length of burst mode data and (2) only for the duration of the element. In both cases we used a 100 Hz frequency box, first centered at 4 kHz and then 4.2 kHz, in both ATH and RBSP A data. We calculated the maximum value of the cross-correlation coefficient using two

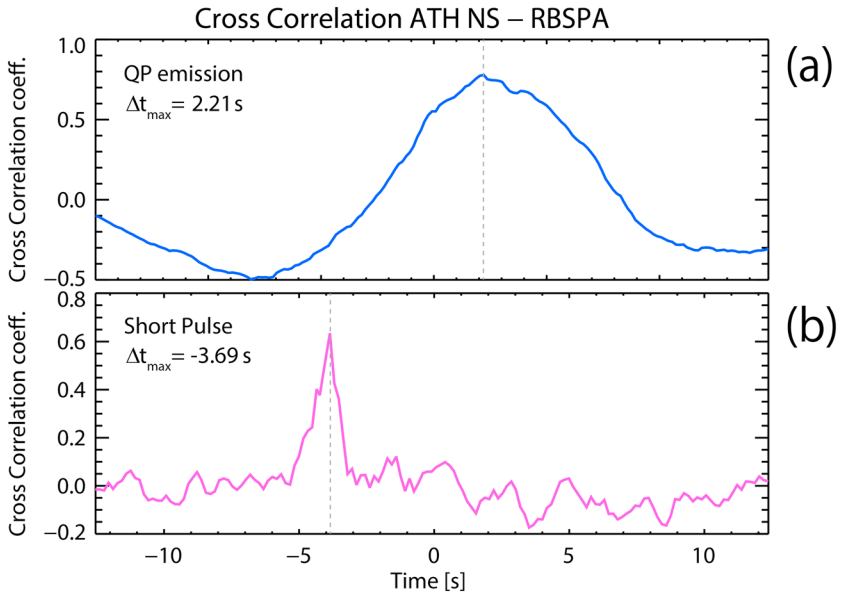

Figure 4. Example of a cross-correlation result for the (a) QP emission and the (b) short pulse.

separate methods: Spearman's rank correlation and Pearson's linear correlation using a similar approach as *Santolík et al.* [2005]. In case (1) we obtained a time delay of +2.13 to +3.77 s, and for case (2) we found +2.21 to +3.85 s. Figure 4a shows an example of the cross correlation, calculated using a 100 Hz box for 4 kHz, as a function of the time delay between the north-south magnetic field component at ATH and B_w component of RBSP A, the delay corresponding to the maximum correlation being indicated in the top left corner. The maximum has a positive time delay in the case of the QP emission, suggesting that ATH saw the VLF emission before RBSP A did. In the case of the SP, we made a similar analysis using a 100 Hz frequency box centered at 4.85 kHz and 4.95 kHz, and a time frame of 10 to 25 s comprising the entirety of the pulse. We obtained a time delay of −3.16 to −3.30 s, using both Spearman and Pearson's coefficients. Figure 4b, in the same format as Figure 4a, shows an example of the cross-correlation coefficient for the frequency box centered at 4.85 kHz and a time frame of 25 s. Contrary to the results obtained for the main QP emission, RBSP A observed the SP before ATH. The time delay values obtained for this conjugate study are consistent with propagation times for whistlers originating at similar L shells [e.g., *Lichtenberger*, 2009] and those calculated for structured ELF hiss [e.g., *Santolik et al.*, 2003a].

3. Discussion

On 25 February 2013, we observed a very rare conjugate event with the same spectral and frequency features on the ground and in space, accompanied by a shorter emission, lasting less than a second and at higher frequencies, of unknown source. The study of this conjugate event has produced interesting observational facts: (1) simultaneous observation of a QP emission accompanied by a short pulse (2) intensity of the emission detected by RBSP A is 1 to 2 orders of magnitude lower than the one detected at ATH (3) even if the QP and the SP are simultaneously observed at both locations; the main QP emission was observed first by ATH, but the SP was detected first by RBSP A. Since the location of the origin of the SP emission is unknown, we decided to concentrate on reproducing the propagation for the main QP emission by assuming that the observed time delay can be explained by a single reflection of the emission from an equatorial source. We consider two ray tracing simulations for the whistler mode waves, the first one back traces the ray from ATH to its probable source location in the geomagnetic equator and the second one follows the ray from the source to the location of RBSP A.

We made preliminary studies using the standard Diffusive Equilibrium (DE) model [*Schunk and Nagy*, 2009] with a dipole model; however, the results gave unrealistic path and group delay values. We then included a density profile gradient by introducing a plasmapause with different widths and locations. Even though these simulations only considered these two parameters of the plasmapause, the results varied greatly, suggesting that as expected, density is one major factor that significantly changes the ray path. We proceeded to fine

tune the simulations by modifying the values of the plasma temperature ($T = 500$, $T = 700$, and $T = 800$ K) and found that even though the ray path differed from case to case, the source location remained globally the same. A detailed explanation of the procedure and results is given in *Martinez-Calderon* [2016].

As the density model distribution plays a fundamental role in ray tracing, we utilized HFR data from the EMFISIS instrument to identify the upper hybrid resonance frequency [*Kurth et al.*, 2015] and obtain a manually fitted cold plasma density profile. Figure 5a shows the manually fitted density profile (blue line) compared with the previously mentioned standard DE model (yellow line) [*Schunk and Nagy*, 2009] with a plasmapause from $L = 5$ to $L = 7$ (maximum *Kp* index of 1+ in the previous 24 h). We observed a few small density peaks from $L = 3.5$ to $L = 4.9$ that we assume represent plasmaspheric ducts close to the observation time of the conjugate event. The location of RBSP A at the time of the event is shown by the gray dashed vertical line and corresponds to a localized decrease of the plasma density suggesting that the observed QP waves propagated in a depletion duct. Figure 5b shows the fitted density distribution in colored background in the meridional plane. Since RBSP was too close to the equator, we could not fit the data with latitudinal dependence, and therefore, the density distribution along the latitudinal plane is taken from the empirical model of [*Denton et al.*, 2004].

For our ray tracing simulation we assume that the trajectory of the wave is invariant to time reversal. In order for the wave to penetrate the lower layers of the ionosphere, the back tracing starting point above ATH should be such that the wave vector $\vec{k}$ is approximately perpendicular to the ground [*Santolik et al.*, 2009]. We also assume that the source of the QP emission is punctual and located at the geomagnetic equatorial plane; thus, the ending point of the back trace is the intersection of the ray and the equatorial plane. However, since RBSP A was located approximately 11° north of the equator, we also consider this difference when taking into account the time delay calculated previously.

We found the source of the emission to be located at relatively low latitudes, $L = 3.4$, inward from the L shells of ATH and RBSP, and with a final angle between the wave vector and the magnetic field line of $\theta_{Bk} \sim 60°$. Previous propagation studies of both chorus and ELF hiss [e.g., *Chum and Santolík*, 2005; *Santolík et al.*, 2006] found that in cases of unducted propagation, large wave vector angles at the equatorial source are needed if the waves are to penetrate the ionosphere. Thus, our results suggest that the waves that propagated directly to ATH did so in an unducted manner. This correlates with previous observations that found that QP waves associated with ULF pulsations observed by Cluster and DEMETER spacecraft propagated unducted with oblique wave normal angles at higher latitudes [i.e., *Němec et al.*, 2013a, 2013b]. The first ray from the source region to ATH is illustrated by the red line in Figure 5b, the red triangle indicates the position of ATH, and the gray arrows represent the direction of $\vec{k}$. The time gap between the arrows being constant (0.09 s and 0.24 s for red and blue ray, respectively), a longer (shorter) distance between the arrows is indicative of the increase (decrease) of group speed.

The propagation from the source to RBSP A is calculated by assuming a punctual source symmetric at the equator, implying that the initial $\vec{k}$ of the waves propagating to the Southern Hemisphere should remain close to 120°. Thus, we sent the waves to the Southern Hemisphere with an initial $\vec{k}$ from 104° to 180° in 1° steps. The trajectory for this ray must have an ending point as close to the actual position of RBSP A as possible, meaning $L = 3.65$ and a magnetic latitude of 10.3°, and also has to reflect the time delay calculations, meaning a group delay between 2.2 and 3.8 s when the wave encounters the satellite. We found that these criteria were met only for an initial wave vector of $\vec{k} \sim 105°$. The resulting wave trajectory corresponds to the dark blue line in Figure 5b, with the dark blue star representing the position of RBSP A at the time of the event. We suggest that the source is constantly emitting waves, some of them propagate unducted to the Northern Hemisphere, directly detected by ATH, while others propagate to the Southern Hemisphere where they are reflected and likely trapped in a depletion duct, as reflected by the density profile, allowing them to be detected by RBSP A. The existence of this small density duct close to the location of the spacecraft is essential in order to obtain the desired group time delay. As a consequence, the final wave vector value has a relatively small significance since when in a duct, the final direction of the wave vector is very variable.

At the time of the event, RBSP A was located in a depletion duct as shown in Figure 5a. Using on-board measurements of the *B* field at the minimum-|*B*| point, we found that the half gyrofrequency ($0.5f_{ce}$) during the entirety of the event was between $6.0 < 0.5f_{ce} < 24.3$ kHz and had a value of approximately $0.5f_{ce}$=12.9 kHz at the time of the QP element. Using Tsyganenko model T01 [i.e., *Tsyganenko*, 2002a, 2002b], we calculated the field line of ATH $0.5f_{ce}$= 4.02 kHz. This correlates with previous studies suggesting that at small wave normal

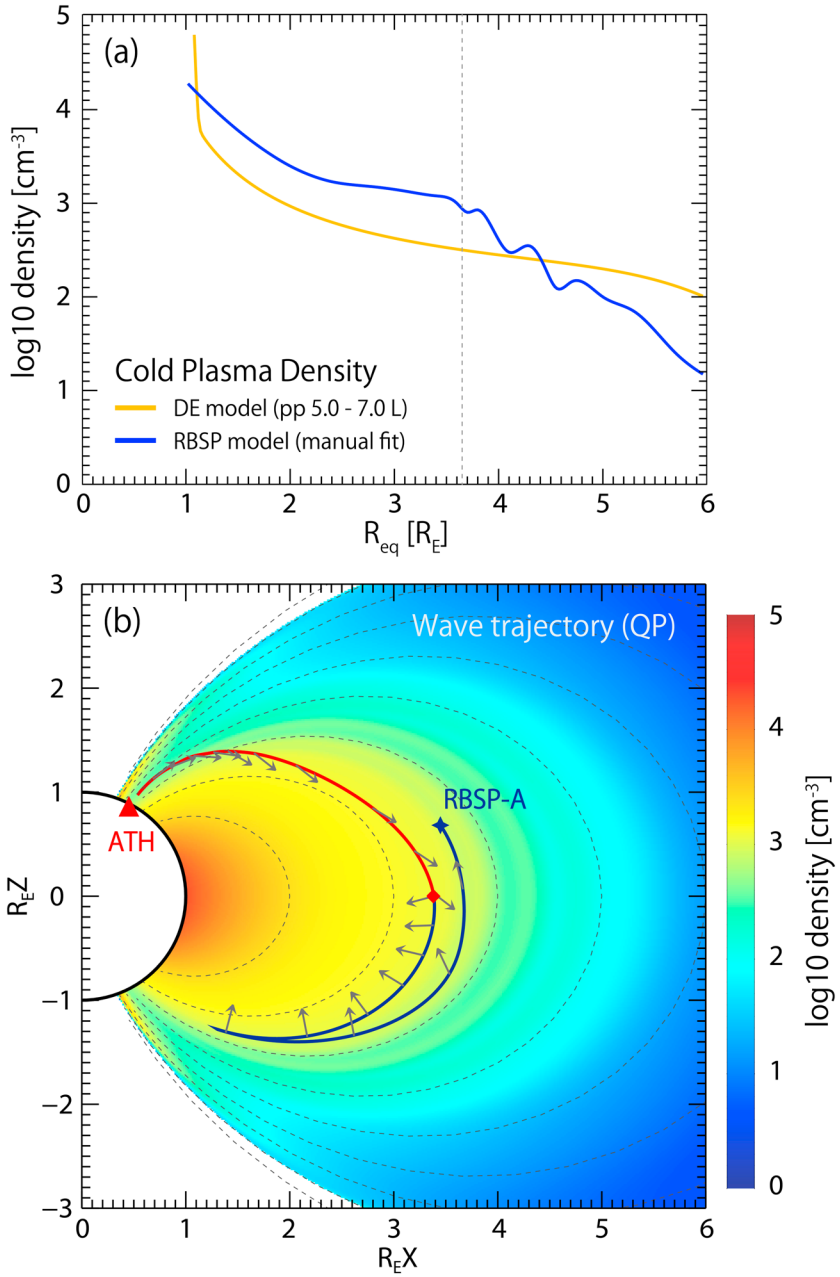

Figure 5. (a) Cold plasma density as a function of R_e; yellow line shows the density profile from the diffusive equilibrium model with a plasmapause from $L = 5$ to 7, while the blue line shows the manually fitted RBSP model. (b) Ray tracing results showing the back trace from ATH (red line) to the source and then the forward trace from RBSP A to the source (blue line).

angles with respect to $\vec{B}_o$ [*Santolik et al.*, 2003a], whistler mode waves with frequencies between $0.5f_{ce}$ and f_{ce} propagate in ducts of depleted cold plasma [e.g., *Bell et al.*, 2009; *Haque et al.*, 2011].

4. Concluding Remarks

In summary, we were able to reproduce, for the first time, ELF/VLF wave propagation based on observational data and with adequate correlation of multiple factors, i.e., spacecraft location, time delay, and Poynting vector. The results of the ray tracing solution presented in this paper indicate that we can accurately reproduce the propagation of the observed waves using current ray tracing models. We found that QP waves

emitted from the same source propagated to the Northern Hemisphere, unducted until they reached the ground at ATH, and also to the Southern Hemisphere, where they reflected and entered a duct allowing them to be detected by RBSP A. These unique results emphasize the importance of actual in situ cold plasma measurements, provided here by RBSP A, in order to accurately reproduce the propagation of VLF/ELF waves.

We have successfully reproduced the observations using ray tracing and a cold plasma density model manually fitted from RBSP A data. We show the ray tracing solution that corresponds the best to the observations and time delay calculations supporting the accuracy of current ray tracing models as well as the important role played by plasma density.

On the other hand, the time delay for the SP cannot be explained if we assume the same propagation as the QP emission. We believe that the source of the SP is located elsewhere in the Southern Hemisphere, and as it propagates through the field line it reaches RBSP A's location first, then continues until being detected by ATH. This is consistent with the calculated time delay from the RBSP A to ATH.

We also found that at subauroral latitudes, the likelihood of conjugate events showing the same frequency and spectral properties between the ground and space remains fairly low (only 1 event out of 77 conjugate RBSP passes). However, we could not determine if this is the consequence of the method employed to select the events or if it is related to ionospheric or magnetospheric propagation of the waves. This could be the subject of future work.

Acknowledgments
The ELF/VLF data are available at the VLF data viewer website from the Institute for Space-Earth Environmental Research (ISEE) accessible at http://stdb2.stelab.nagoya-u.ac.jp/vlf/index2.html. We would like to thank Y. Katoh, H. Hamaguchi, Y. Yamamoto, and T. Adachi of ISEE, as well as K. Reiter from Athabasca University, for their continued technical support. The construction and operation of the Athabasca University Geophysical Observatory facilities are supported by the Canada Foundation for Innovation. Tsyganenko model calculations were done using the IDL Geopack Dynamic Link Module (DLM) routines by H. Korth, providing access to the GEOPACK Fortran library by N.A. Tsyganenko (http://ampere.jhuapl.edu/code/idl_geopack.html) and based on solar wind parameters from the OMNI database provided by the SPDF/GSFC OMNIWeb interface (http://omniweb.gsfc.nasa.gov/form/omni_min.html). The Conjugate Event Finder can be accessed at http://gemsissc.stelab.nagoya-u.ac.jp/cef/cef.cgi? at the ERG science center. This work was supported by the Inter-university Upper atmosphere Global Observation NETwork (IUGONET) of the Japanese Ministry of Education, Culture, Sports, Science and Technology (MEXT). We were also supported by the Grant-in-Aid for Scientific Research (20244080, 23403009, 23340146, 25302006, 25247080, 15H05747, 15H05815, and 16H06286) from the Japan Society for the Promotion of Science and by the Leadership Development Program for Space Exploration and Research at Nagoya University. K. Keika is supported by the GEMSIS project at ISEE, and part of his work was done at the ERG-Science Center operated by ISAS/JAXA and ISEE/Nagoya University. The work done at the Charles University and at the Institute of Atmospheric Physics in Prague has been supported from the LH14010 and GACR14-31899S grants.

References

Barr, R., D. L. Jones, and C. Rodger (2000), ELF and VLF radio waves, *J. Atmos. Sol. Terr. Phys.*, *62*(17), 1689–1718.
Bell, T. F., U. S. Inan, N. Haque, and J. Pickett (2009), Source regions of banded chorus, *Geophys. Res. Lett.*, *36*(L11101), doi:10.1029/2009GL037629.
Bortnik, J., and R. Thorne (2007), The dual role of ELF/VLF chorus waves in the acceleration and precipitation of radiation belt electrons, *J. Atmos. Sol. Terr. Phys.*, *69*(3), 378–386.
Chum, J., and O. Santolík (2005), Propagation of whistler-mode chorus to low altitudes: Divergent ray trajectories and ground accessibility, *Ann. Geophys.*, *23*(12), 3727–3738, doi:10.5194/angeo-23-3727-2005.
Denton, R., J. Menietti, J. Goldstein, S. Young, and R. Anderson (2004), Electron density in the magnetosphere, *J. Geophys. Res.*, *109*, A09215, doi:10.1029/2003JA010245.
Haque, N., U. S. Inan, T. F. Bell, J. S. Pickett, J.-G. Trotignon, and G. Facskó (2011), Cluster observations of whistler mode ducts and banded chorus, *Geophys. Res. Lett.*, *38*, L18107, doi:10.1029/2011GL049112.
Hayosh, M., D. L. Pasmanik, A. G. Demekhov, O. Santolik, M. Parrot, and E. E. Titova (2013), Simultaneous observations of quasi-periodic ELF/VLF wave emissions and electron precipitation by DEMETER satellite: A case study, *J. Geophys. Res. Space Physics*, *118*, 4523–4533, doi:10.1002/jgra.50179.
Hayosh, M., F. Nemec, O. Santolik, and M. Parrot (2014), Statistical investigation of VLF quasiperiodic emissions measured by the DEMETER spacecraft, *J. Geophys. Res. Space Physics*, *119*, 8063–8072, doi:10.1002/2013JA019731.
Helliwell, R. A. (1965), *Whistlers and Related Ionospheric Phenomena*, vol. 1, Stanford Univ. Press, Stanford, Calif.
Horne, R. B., et al. (2005), Wave acceleration of electrons in the Van Allen radiation belts, *Nature*, *437*(7056), 227–230.
Kitamura, T., J. Jacobs, T. Watanabe, and R. B Flint (1968), Investigation of quasi-periodic VLF emissions and their relation to geomagnetic micropulsations, *Nature*, *220*, 360–361.
Kletzing, C., et al. (2013), The Electric and Magnetic Field Instrument Suite and Integrated Science (EMFISIS) on RBSP, in *The Van Allen Probes Mission*, vol. 179, pp. 127–181, Springer, Netherlands.
Kurth, W., S. De Pascuale, J. Faden, C. Kletzing, G. Hospodarsky, S. Thaller, and J. Wygant (2015), Electron densities inferred from plasma wave spectra obtained by the waves instrument on Van Allen Probes, *J. Geophys. Res. Space Physics*, *120*(2), 904–914, doi:10.1002/2014JA020857.
Lauben, D. S., U. S. Inan, T. F. Bell, and D. Gurnett (2002), Source characteristics of ELF/VLF chorus, *J. Geophys. Res.*, *107*(A12), 1429, doi:10.1029/2000JA003019.
Lichtenberger, J. (2009), A new whistler inversion method, *J. Geophys. Res.*, *114*, A07222, doi:10.1029/2008JA013799.
Lyons, L. R., R. M. Thorne, and C. F. Kennel (1972), Pitch-angle diffusion of radiation belt electrons within the plasmasphere, *J. Geophys. Res.*, *77*(19), 3455–3474, doi:10.1029/JA077i019p03455.
Martinez-Calderon, C., K. Shiokawa, Y. Miyoshi, M. Ozaki, I. Schofield, and M. Connors (2015a), Polarization analysis of VLF/ELF waves observed at subauroral latitudes during the VLF-CHAIN campaign, *Earth, Planets Space*, *67*(1), 1–13.
Martinez-Calderon, C., K. Shiokawa, Y. Miyoshi, M. Ozaki, I. Schofield, and M. Connors (2015b), Statistical study of ELF/VLF emissions at subauroral latitudes in Athabasca, Canada, *J. Geophys. Res. Space Physics*, *120*, 8455–8469, doi:10.1002/2015JA021347.
Martinez-Calderon, C. (2016), Study of magnetospheric ELF/VLF waves at subauroral latitudes using ground-based and spacecraft observations, PhD Thesis, p. 108, Nagoya Univ., Nagoya, Japan.
Meredith, N. P., R. B. Horne, R. M. Thorne, and R. R. Anderson (2003), Favored regions for chorus-driven electron acceleration to relativistic energies in the Earth's outer radiation belt, *Geophys. Res. Lett.*, *30*(16), doi:10.1029/2003GL017698.
Miyashita, Y., I. Shinohara, M. Fujimoto, H. Hasegawa, K. Hosokawa, T. Takada, and T. Hori (2011), A powerful tool for browsing quick-look data in solar-terrestrial physics: Conjunction Event Finder, *Earth, Planets Space*, *63*(1), e1—e4.
Miyoshi, Y., A. Morioka, H. Misawa, T. Obara, T. Nagai, and Y. Kasahara (2003), Rebuilding process of the outer radiation belt during the 3 November 1993 magnetic storm: NOAA and EXOS-D observations, *J. Geophys. Res.*, *108*(A1), 1004, doi:10.1029/2001JA007542.
Miyoshi, Y., et al. (2015), Relation between fine structure of energy spectra for pulsating aurora electrons and frequency spectra of whistler-mode chorus waves, *J. Geophys. Res. Space Physics*, *120*, 7728–7736, doi:10.1002/2015JA021562.
Němec, O., M. Santolík, F. Parrot, J. Pickett, M. Hayosh, and N. Cornilleau-Wehrlin (2013a), Conjugate observations of quasi-periodic emissions by Cluster and DEMETER spacecraft, *J. Geophys. Res. Space Physics*, *118*(1), 198–208, doi:10.1029/2012JA018380.

Němec, O., F. Santolík, J. Pickett, M. Parrot, and N. Cornilleau-Wehrlin (2013b), Quasiperiodic emissions observed by the Cluster spacecraft and their association with ULF magnetic pulsations, *J. Geophys. Res. Space Physics*, *118*(1), 4210–4220, doi:10.1002/jgra.50406.

Němec, F., J. Pickett, and O. Santolík (2014), Multispacecraft cluster observations of quasiperiodic emissions close to the geomagnetic equator, *J. Geophys. Res. Space Physics*, *119*(11), 9101–9112, doi:10.1002/2014JA020321.

Ozaki, M., S. Yagitani, I. Nagano, Y. Hata, H. Yamagishi, N. Sato, and A. Kadokura (2008), Localization of VLF ionospheric exit point by comparison of multipoint ground-based observation with full-wave analysis, *Polar Sci.*, *2*(4), 237–249.

Santolik, O., F. Lefeuvre, M. Parrot, and J. Rauch (2001), Complete wave-vector directions of electromagnetic emissions: Application to interball-2 measurements in the nightside auroral zone, *J. Geophys. Res.*, *106*(A7), 13,191–13,201.

Santolik, O., D. Gurnett, J. Pickett, M. Parrot, and N. Cornilleau-Wehrlin (2003a), Spatio-temporal structure of storm-time chorus, *J. Geophys. Res.*, *108*(A7), 1278, doi:10.1029/2002JA009791.

Santolík, O., M. Parrot, and F. Lefeuvre (2003b), Singular value decomposition methods for wave propagation analysis, *Radio Sci.*, *38*, 1010, doi:10.1029/2000RS002523.

Santolík, O., A. Persoon, D. Gurnett, P. Decreau, J. Pickett, O. Marsšálek, M. Maksimovic, and N. Cornilleau-Wehrlin (2005), Drifting field-aligned density structures in the night-side polar cap, *Geophys. Res. Lett.*, *32*, L06106, doi:10.1029/2004GL021696.

Santolík, O., J. Chum, M. Parrot, D. Gurnett, J. Pickett, and N. Cornilleau-Wehrlin (2006), Propagation of whistler mode chorus to low altitudes: Spacecraft observations of structured ELF hiss, *J. Geophys. Res.*, *111*, A10208, doi:10.1029/2005JA011462.

Santolik, O., M. Parrot, U. Inan, D. Buresšová, D. Gurnett, and J. Chum (2009), Propagation of unducted whistlers from their source lightning: A case study, *J. Geophys. Res.*, *114*, A03212, doi:10.1029/2008JA013776.

Sato, N., K. Hayashi, S. Kokubun, T. Oguti, and H. Fukunishi (1974), Relationships between quasi-periodic VLF emission and geomagnetic pulsation, *J. Atmos. Terr. Phys.*, *36*, 1515–1526.

Sazhin, S., and M. Hayakawa (1994), Periodic and quasiperiodic VLF emissions, *J. Atmos. Terr. Phys.*, *56*(6), 735–753.

Schunk, R., and A. Nagy (2009), *Ionospheres: Physics, Plasma Physics, and Chemistry*, Cambridge Univ. Press, Cambridge, U. K.

Shiokawa, K. et al. (2014), Ground-based ELF/VLF chorus observations at subauroral latitudes—VLF-CHAIN campaign, *J. Geophys. Res. Space Physics*, *119*(9), 7363–7379, doi:10.1002/2014JA020161.

Titova, E., B. Kozelov, A. Demekhov, J. Manninen, O. Santolik, C. Kletzing, and G. Reeves (2015), Identification of the source of quasiperiodic VLF emissions using ground-based and Van Allen Probes satellite observations, *Geophys. Res. Lett.*, *42*, 6137–6145, doi:10.1002/2015GL064911.

Tsyganenko, N. A. (2002a), A model of the near magnetosphere with a dawn-dusk asymmetry 1. Mathematical structure, *J. Geophys. Res.*, *107*(A8), 1179, doi:10.1029/2001JA000220.

Tsyganenko, N. A. (2002b), A model of the near magnetosphere with a dawn-dusk asymmetry 2. Parameterization and fitting to observations, *J. Geophys. Res.*, *107*(A8), 1176, doi:10.1029/2001JA000220.